

EFFECT OF MICROSTRUCTURE ON FATIGUE CRACK GROWTH RATE

OF ALLOY 718 AT 650°C

A.K. Koul and J.-P. Immarigeon

Structures and Materials Laboratory  
National Aeronautical Establishment  
National Research Council of Canada  
Ottawa, Ontario, Canada

Abstract

This paper examines the influence of serrated grain boundary morphology and dislocation substructures on the fatigue crack growth resistance of Alloy 718 at 650°C in laboratory air. The serrated grain boundary work was conducted on experimental plate stock whereas the influence of dislocation substructures was examined on specimens machined from service exposed discs that were retrieved from aero engines.

Serrated grain boundaries retard the fatigue crack growth rates (FCGR's) by suppressing grain boundary sliding and providing a tortuous path for crack growth. The influence of dislocation substructures on FCGR's can vary markedly with the type of substructure present. High dislocation densities in the form of planar arrays dramatically increase the FCGR's relative to cellular dislocation arrangements. The origin of dislocation substructures in relation to remnant forging strains or service induced LCF damage is considered in detail. The influence of stress cycling on substructure development in service exposed discs is also discussed.

## Introduction

The influence of microstructure on the elevated temperature fatigue crack growth rate (FCGR) in Alloy 718 has been investigated by a number of research workers in recent years. These investigations have primarily concentrated on the effects of microstructural variables such as grain size, intragranular body centered tetragonal  $\text{Ni}_3\text{Nb}$  ( $\gamma''$ ) precipitate size and orthorhombic  $\text{Ni}_3\text{Nb}$  ( $\delta$ ) needle distribution at the grain boundaries.(1-6) In general, it has been found that a coarse grain size improves FCGR resistance whereas a fine  $\gamma''$  precipitate size increases FCGR's at temperatures in the vicinity of 400 to 650°C in laboratory air. Mills and James (4) have also found that Laves and  $\delta$  particles enhance microvoid nucleation ahead of the advancing crack front which in turn accelerates the FCGR at intermediate and high stress intensity ranges ( $\Delta K$ ) at 649°C. Recent work by Thamburaj et al. (5) and Koul et al (7) has however shown that a profusely serrated grain boundary structure can be produced in Alloy 718 through the precipitation of a limited amount of grain boundary  $\delta$  phase in well controlled heat treatments. A serrated grain boundary morphology can be usefully exploited to suppress grain boundary sliding and to improve the elevated temperature FCGR resistance of this alloy. One of the objectives of the present paper is to expound on the influence of serrated grain boundaries on FCGR's.

While it has been established that grain size,  $\gamma''$  precipitate size and  $\delta$  phase distribution strongly influence the FCGR's in Alloy 718, there is very little information on the effects of dislocation substructures on FCGR's in this alloy. Dislocation substructures can either be introduced during forging of the material or during cyclic straining of gas turbine engine components such as compressor and turbine discs. Therefore, another objective of this paper is to analyze the effect of dislocation substructures on FCGR's in service exposed Alloy 718 turbine discs.

## Experimental Materials and Methods

The commercially available hot rolled Alloy 718 was procured in the form of 12.7 mm thick x 50.8 mm wide plates and the chemical composition of this material is given in Table 1. The plate stock was used for studying the influence of serrated grain boundaries on FCGR's at 650°C.

Alloy 718 material was also obtained in the form of two retired first stage turbine discs, from an aero engine, with service time since new (TSN) of 1520 hours (referred to as the medium TSN disc) and 2045 hours (referred to as the high TSN disc) respectively. The material for both discs came from the same alloy heat and these discs had also been forged from a single billet stock. The chemical composition of the alloy heat conformed to the specifications given in Table 1.

## Heat Treatments and Microscopy

Two different heat treatments, named "Merrick" and "Modified Merrick", were applied to the plate material prior to machining the fracture mechanics specimens. The details of these heat treatments are given in Table 2. The "Merrick" heat treatment has been previously developed by other investigators (8) whereas the "Modified Merrick" heat treatment was developed in the authors' laboratory (3,5). Both heat treatments start with a solution treatment at 1066°C for 1 hour followed by intermediate aging at 843°C for 4 hours and the standard double aging treatment. In the case of the "Merrick" heat treatment the intermediate aging is carried out

TABLE 1: Chemical Compositions and Specifications of Alloy 718 Experimental Materials

Material Stock	C	Si	Cr	Ni	Mo	Nb & Ta	Ti	Al
Plate	0.05	0.21	17.9	53.1	3.06	5.11	0.96	0.47
Turbine Discs	0.02/0.08	0.35 max.	17/21	50/55	2.8/3.3	4.75/5.50	0.75/1.15	0.3/0.7

TABLE 2: Summary of "Merrick" and "Modified Merrick" Heat Treatment Schedules and the Overall Microstructural Features

Heat Treatment	Heat Treatment Schedule	Microstructural Features		
		Grain Size $\mu\text{m}$	Relative $\gamma$ " Size	Grain Boundary Morphology
Merrick	1066°C/1h+843°C/4h+ 718°C/8h $\xrightarrow{1^\circ\text{C}/\text{min}}$ 621°C/10h/AC	50 - 120	Coarse	Planar
Modified Merrick	1066/1h $\xrightarrow{7^\circ\text{C}/\text{min}}$ 843°C/4h+718°C/8h $\xrightarrow{1^\circ\text{C}/\text{min}}$ 621°C/10h/AC	50 - 120	Fine	Serrated

directly after the solution treatment whereas the "Modified Merrick" heat treatment employs a furnace cool of  $\sim 7^{\circ}\text{C}$  /minute to the intermediate aging temperature. In the "Modified Merrick" heat treatment, the furnace cooling together with intermediate aging at  $843^{\circ}\text{C}$  for 4 hours produce profuse serration at the grain boundaries whereas the "Merrick" heat treatment essentially produces a planar grain boundary morphology, Fig. 1.

The service exposed discs tested in the present study had been machined from the forged stock and these forgings had been solution treated at  $954^{\circ}\text{C}$  for 1 hour followed by the standard double aging treatment. These discs were not subjected to any post-service heat treatments and the fracture mechanics specimens from the discs were directly machined from the as-retrieved components.

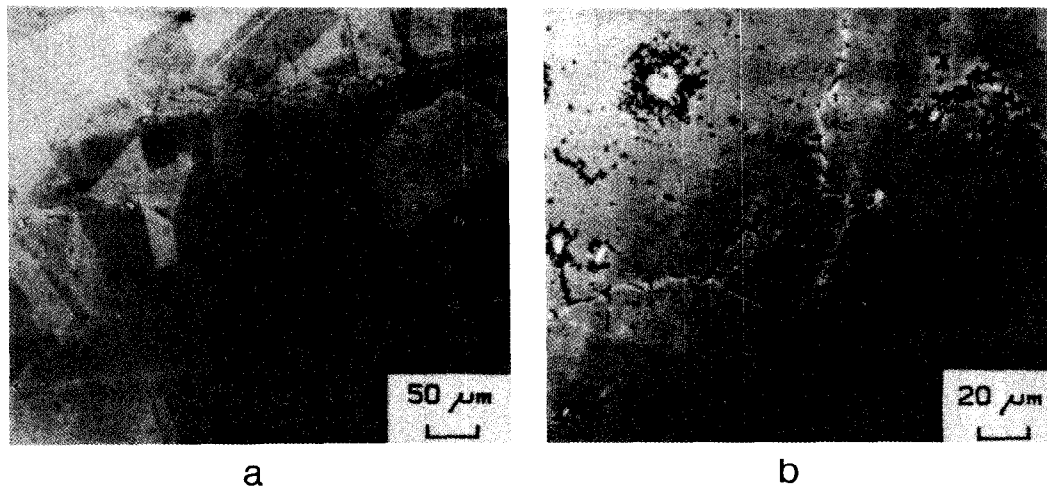


Fig. 1 Effect of "Merrick" and "Modified Merrick" heat treatments on the grain boundary structure of Alloy 718. (a) Merrick, and (b) Modified Merrick, heat treated materials.

Standard metallographic procedures were used to prepare the experimental plate and the service exposed disc specimens for optical microscopy. The specimens were etched in a solution composed of 2 parts water, 1 part hydrogen peroxide solution (30% solution) and 3 parts hydrochloric acid to reveal the microstructure. The ASTM mean linear intercept method was used to determine the average grain size of the etched specimens. In the case of the service exposed discs, the average grain size from bore to rim was determined by examining samples removed from radial sections of each disc.

Thin foils, for transmission electron microscopy (TEM), were prepared by twin jet thinning in an electrolyte consisting of 94 parts acetic acid and 6 parts perchloric acid by volume. These foils were used to characterize the distributions of  $\gamma'$ ,  $\gamma''$  and  $\delta$  phases and dislocation structures in both heat treated plate stock as well as the service exposed discs.

## Fracture Mechanics Testing

All FCGR tests were conducted in electrohydraulic test systems. Tapered double cantilever beam (DCB) fracture mechanics specimens, having a constant stress intensity region over 31 mm (5), were machined from the heat treated plate stock, Fig. 2. The FCGR tests on DCB specimens were conducted at constant  $\Delta K$  values of 45 and 90 MPa  $\sqrt{\text{m}}$  in laboratory air at 650°C. The stress ratio (R) of 0.1 and a frequency of 0.1 Hz were used for DCB specimen testing using a sine wave form. Fracture surfaces were studied by scanning electron microscopy (SEM) to determine the crack growth rates and failure modes.

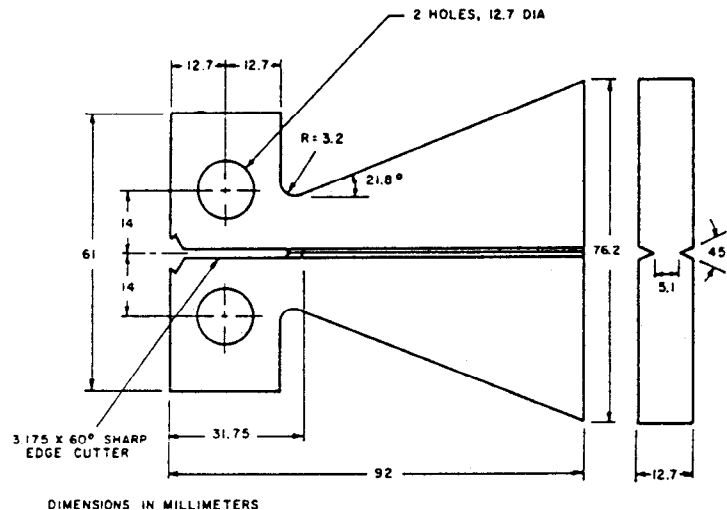


Fig. 2 Dimensions of tapered double cantilever beam specimen (DCB) used for FCGR testing. (After Thamburaj et al. Ref. 5)

To investigate the effects of dislocation substructures on fracture mechanics properties of Alloy 718, FCGR testing was performed on compact tension (CT) specimens machined from the service exposed discs. It is already known that bolt hole regions accumulate maximum damage due to stress cycling and are the fracture critical locations in these discs (9). Therefore, CT specimens were machined as close to the bolt holes as possible, Fig. 3. The CT specimens were machined in a manner such that the direction of crack propagation through the specimen was radial towards the bore of the disc. This orientation is also illustrated in Fig. 3. The geometry of the CT specimens used in this work is given in Fig. 4. The CT specimen met the ASTM standard E-647-83 minimum size recommendations in all dimensions (10). The specimen thickness was dictated by the minimum disc thickness in the bolt hole region and this corresponds to the 4.75 mm (0.187 in) dimension in Fig. 4. The CT specimen required a precrack of 6.67 mm and the final crack length was taken as 14.43 mm in order to meet the elasticity requirements as specified in ASTM standard E-647-83 (10). These crack lengths correspond to a  $\Delta K$  range of 30 to 72 MPa  $\sqrt{\text{m}}$  at an R value of 0.1. The FCGR testing was carried out at 650°C in laboratory air using a sawtooth waveform at a frequency of 1 Hz. An automated direct current potential drop (DC-PD) technique, with a precision of 0.025 mm was used to monitor the crack lengths during testing (11). The data acquisition time for the DC-PD technique was limited to 0.5 seconds per

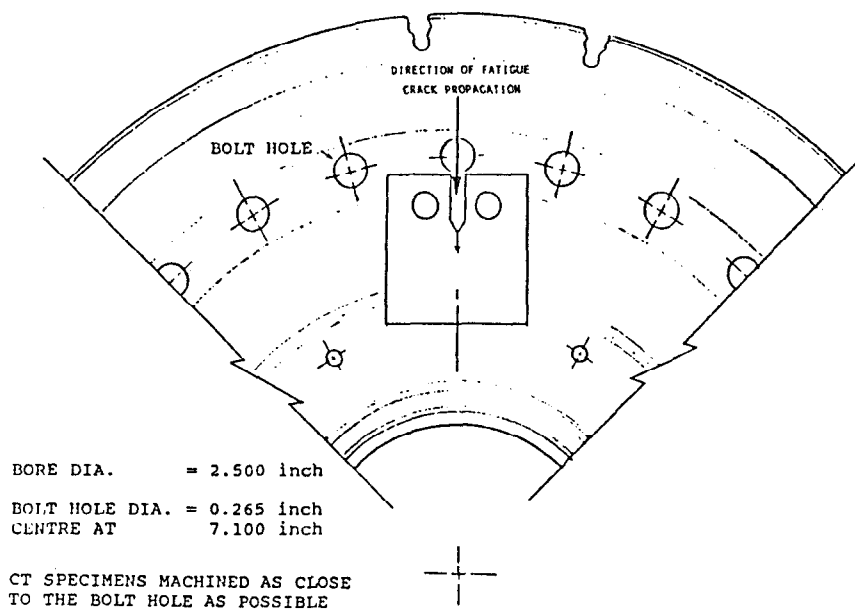


Fig. 3 Location of the compact tension (CT) specimens machined from Alloy 718 turbine discs.

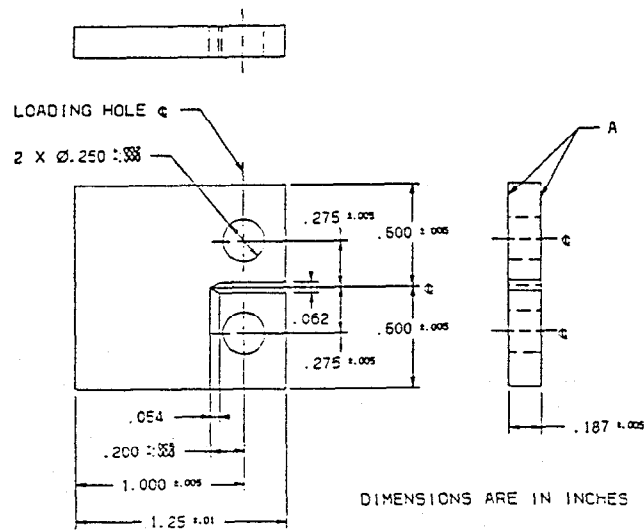


Fig. 4 Dimensions of the CT specimens machined from turbine discs.

data acquisition sequence in order to minimize the contribution of creep towards crack growth. Four CT specimens from each service exposed disc were tested. The SEM examination of the fracture surfaces was carried out to elucidate the failure modes.

## Results

### Alloy 718 Plate Stock

The results of optical and TEM examination of Alloy 718 subjected to "Merrick" and "Modified Merrick" heat treatments are compared in Table 2 and Figs. 1 and 5. The grain sizes produced by the two heat treatments are similar although their grain boundary morphologies and intragranular  $\gamma$  precipitate sizes differ markedly. The "Merrick" heat treatment produces a coarse  $\gamma$  precipitate distribution and a planar grain boundary structure whereas the "Modified Merrick" heat treatment results in a fine  $\gamma$  precipitate size and a profusely serrated grain boundary morphology.

The FCGR's of the "Merrick" and "Modified Merrick" heat treated materials at  $45 \text{ MPa} \sqrt{\text{m}}$  and  $90 \text{ MPa} \sqrt{\text{m}}$  in air environment at  $650^\circ\text{C}$  are compared in Table 3. The crack growth resistance of the "Modified Merrick" heat treated material is superior to that of the "Merrick" heat treated material at both stress intensity ranges. Although the fracture modes in

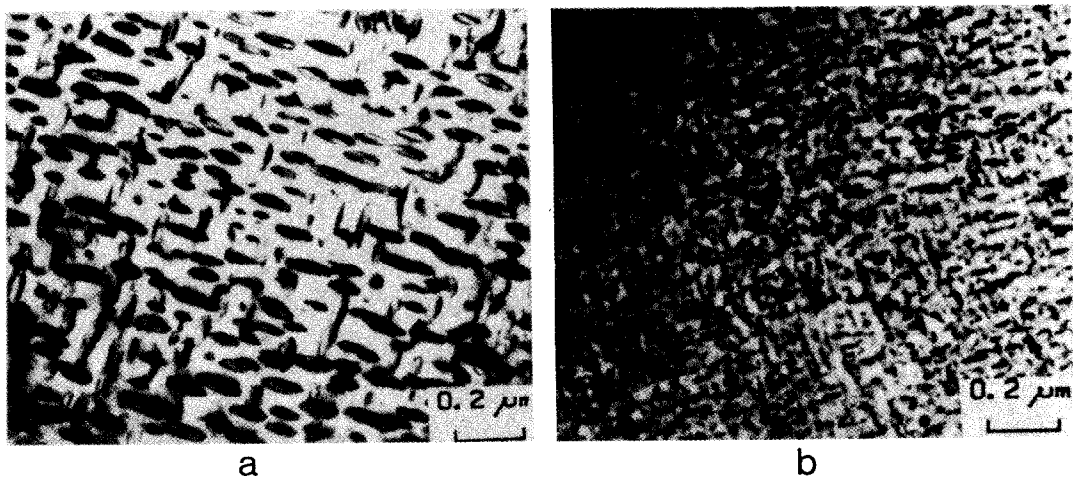
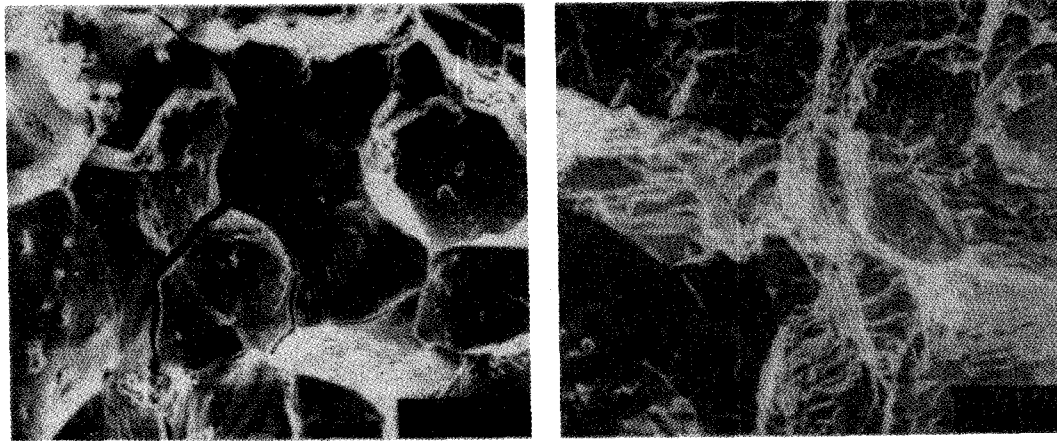


Fig. 5 Effect of "Merrick" and "Modified Merrick" heat treatments on the  $\gamma$  precipitate size and distribution in Alloy 718. (a) Merrick, and (b) Modified Merrick heat treated materials.

TABLE 3: Influence of Serrated Grain Boundaries on FCGR's in Alloy 718 at  $650^\circ\text{C}$  in Laboratory Air

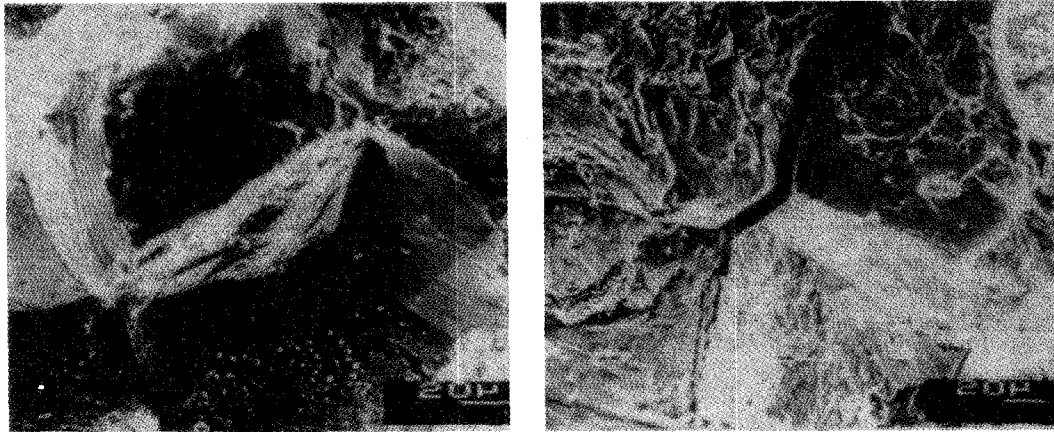
Heat Treatment	Fatigue Crack Growth Rates in Air in $\text{mm}/\text{cycle} \times 10^{-3}$ at	
	$45 \text{ MPa} \sqrt{\text{m}}$	$90 \text{ MPa} \sqrt{\text{m}}$
Merrick	2.7	12.0
Modified Merrick	2.0	7.21



a

b

Fig. 6 Fracture modes of Alloy 718 at  $45 \text{ MPa} \sqrt{\text{m}}$  at  $650^\circ\text{C}$  in laboratory air. (a) Merrick, and (b) Modified Merrick heat treated materials.



a

b

Fig. 7 Fracture modes of Alloy 718 at  $90 \text{ MPa} \sqrt{\text{m}}$  at  $650^\circ\text{C}$  in laboratory air. (a) Merrick, and (b) Modified Merrick heat treated materials.

both microstructures were intergranular at both stress intensity ranges, Figs. 6 and 7, the "Merrick" treated material showed sharp grain boundary facets whereas in "Modified Merrick" heat treated material grain boundary facets revealed stair-step appearance including the presence of some ductile features.

#### Alloy 718 Turbine Discs

The average grain sizes of both medium and high TSN discs, in locations where fracture mechanics specimens were machined from, were  $\sim 15 \mu\text{m}$  although the individual grains varied in size from  $3$  to  $60 \mu\text{m}$ . The hardness values in both discs tended to remain constant over the entire radial distance from bore to rim. The average hardness values in CT specimen locations in both discs were around  $R_c45$ .



The TEM observations revealed that there were no essential differences in the  $\gamma'$  and  $\gamma''$  precipitate sizes and distributions between the medium and the high TSN discs, Fig. 8. The high TSN disc, however, revealed the presence of a large number of intragranular planar dislocation arrays, Fig. 9(a), and low angle boundaries, Fig. 9(b), in the bolt hole and bore regions respectively. In contrast, the dislocation array arrangements in the medium TSN disc were cellular, Fig. 10, and there was no indication of low angle boundary formation in any region of this disc. The  $\gamma'$  and  $\gamma''$  precipitates in the vicinity of these dislocation substructures in both discs did not reveal any unusual features such as coarser  $\gamma''$  precipitates along dislocation lines. These observations indicate that these dislocation substructures had probably formed during service in both discs.

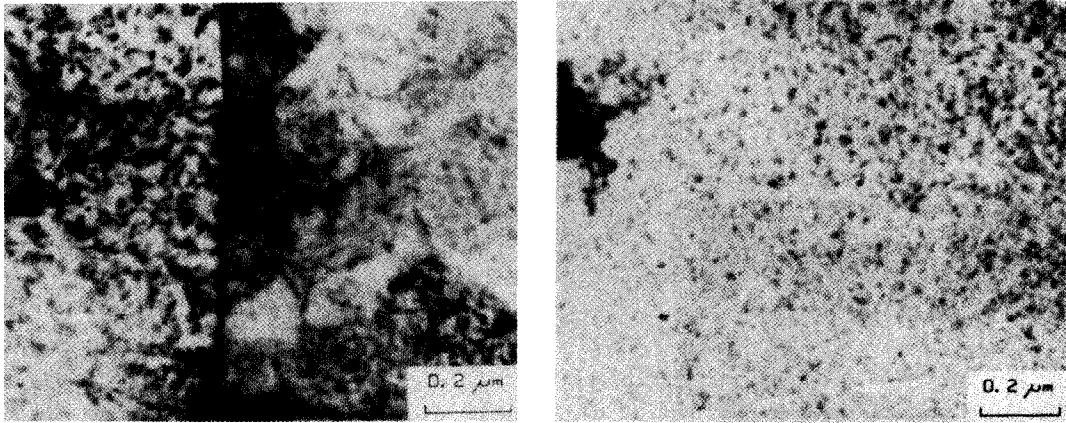


Fig. 8 Transmission electron micrographs of service exposed Alloy 718 discs showing typical  $\gamma''$  sizes and distributions. (a) Medium TSN disc and (b) High TSN disc. (After Pishva et al. Ref. 9)

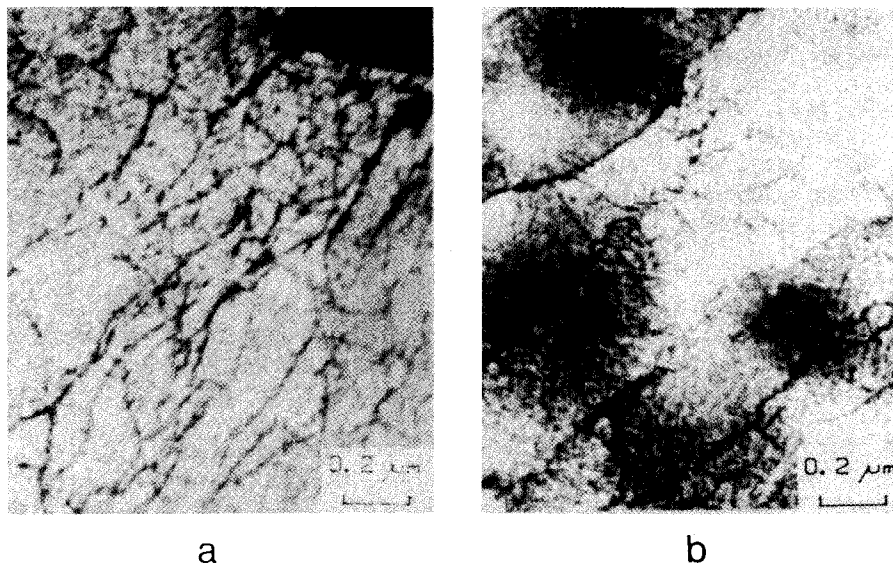


Fig. 9 Typical dislocation structures observed in the high TSN Alloy 718 disc. (a) CT specimen location (bolt hole regions) and (b) bore region. (After Pishva et al. Ref. 9)

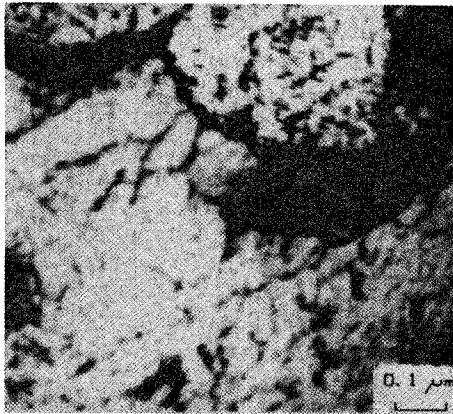


Fig. 10 Typical dislocation structures observed in the medium TSN Alloy 718 disc. (After Pishva et al. Ref. 9)

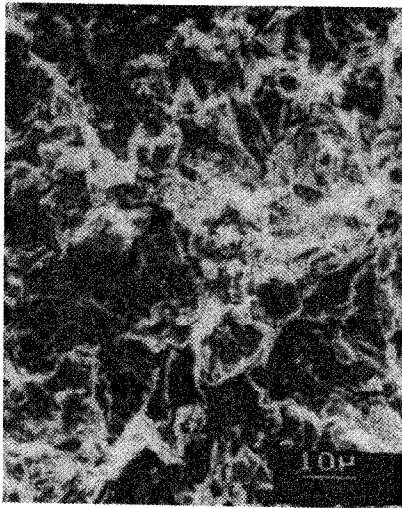


Fig. 12 Typical fracture mode observed in Alloy 718 CT specimens machined from service exposed turbine discs.

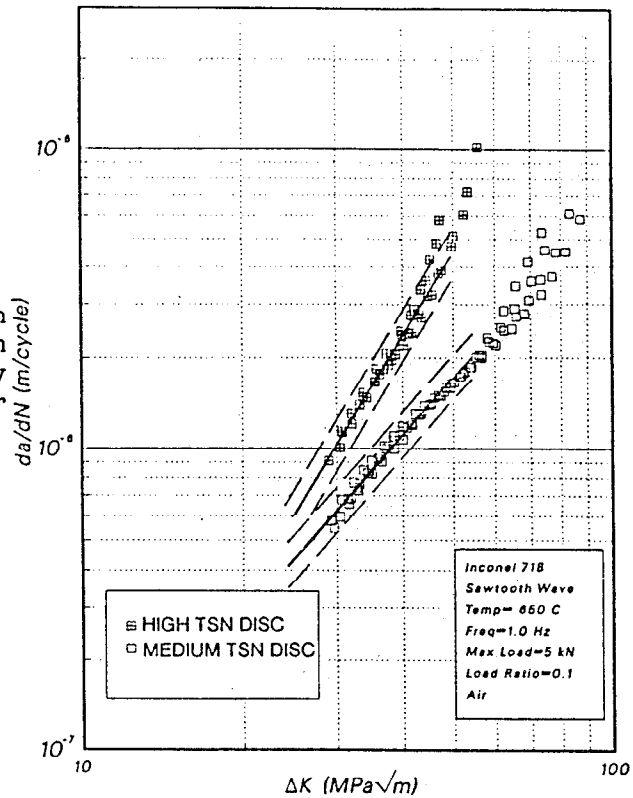


Fig. 11 The FCGR data generated on CT specimens machined from medium and high TSN Alloy 718 discs at 650°C in air environment. (After Pishva et al. Ref. 9)

The FCGR data generated on CT specimens from the medium and high TSN discs showed a large amount of scatter and these data are compared in Fig. 11. The solid lines and the two parallel dashed lines in Fig. 11 represent the mean line and the  $\pm 3$  conditional standard deviations from the mean within Paris regime of crack growth. Relative to the medium TSN disc, the high TSN disc specimens revealed FCGR's that were higher by a factor of 2 to 5 over a  $\Delta K$  range of 30 - 55  $\text{MPa}\sqrt{\text{m}}$ , Fig. 11. The FCGR data within the tertiary regimes of crack growth indicate that the fracture toughness of the medium TSN disc is considerably higher than the high TSN disc.

The SEM examination of the cracked CT specimens from both discs revealed a mixed intergranular and transgranular mode of fracture, Fig. 12, indicating that the differences in dislocation substructures do not influence the actual failure mechanism.

## Discussion

### Effect of Serrated Grain Boundaries on FCGR's

The "Modified Merrick" heat treated material contained very fine  $\gamma''$  precipitates relative to the "Merrick" heat treated material. Recent work by Krueger, Antolovich and Van Stone (6) on Alloy 718 suggests that smaller  $\gamma''$  precipitates suppress dislocation reversal within the plastic zone and this reduced reversibility causes damage to accumulate faster which results in rapid crack propagation during stage II cracking. In addition, there is ample indirect evidence for an inverse relationship between matrix  $\gamma'$  or  $\gamma''$  precipitate size and the sensitivity to environmental embrittlement in Alloy 718 (5, 12). When the matrix precipitate size is relatively fine, intense stress concentrations occur at the grain boundaries because dislocation motion within the grain interiors is impeded. If at the same time grain boundary cohesive strength and mobility is reduced as a result of adsorption of aggressive environmental species, intergranular cracking would be promoted under grain boundary sliding conditions (5,12,13). Despite the presence of fine  $\gamma''$  precipitates in "Modified Merrick" heat treated material, its fatigue crack growth resistance is marginally superior to that of the "Merrick" heat treated material at 650°C in air environment, Table 3. It is thus concluded that the presence of a serrated grain boundary morphology in the "Modified Merrick" heat treated material offsets the detrimental effect of a finer  $\gamma''$  precipitate size by suppressing grain boundary sliding under FCGR conditions at 650°C in Alloy 718.

The suppression of grain boundary sliding within the plastic zone ahead of the crack tip forces deformation to occur within the grain interiors which relieves grain boundary stress concentrations and retards crack growth at elevated temperatures. Indirect evidence for this effect can be seen in creep testing results of the "Merrick" and "Modified Merrick" heat treated materials, Table 4, where the presence of serrations clearly improves the creep ductility of Alloy 718 at 650°C. In addition, recent work by Tanaka, Iizuka and Ashihara (14) on creep crack growth in heat-resisting austenitic steels suggests that angular grain boundary serrations (similar to those found in Alloy 718) deflect the crack and arrest a growing crack at the point of inflection of a serration which in turn retard crack growth. The fracture morphology of the FCGR tested "Modified Merrick" heat treated material supports both arguments because fractured grain boundary facets show the presence of "stair-steps" along with some ductile features, Figs. 5 and 6. These observations indicate that a fatigue crack in the "Modified Merrick" heat treated Alloy 718

TABLE 4: Effect of Microstructures on Creep Properties  
in Alloy 718 at 690 MPa and 650°C

Heat Treatment	Rupture Life in h	% Rupture Elongation
Merrick	160 - 179	1.87 - 3.53
Modified Merrick	154 - 190	5.80 - 6.43

indeed follows a tortuous path along the grain boundaries and, in addition, some deformation also occurs in matrix regions immediately adjacent to the serrated grain boundaries.

## Effect of Dislocation Substructures on FCGR's

Literature contains limited information on the effects of dislocation substructures on FCGR's in Ni-base superalloys. This is because Ni-base superalloy microstructures are very complex which makes it difficult to systematically analyze the dislocation substructure effects on elevated temperature mechanical properties.

In the present study, however, the medium and high TSN discs were manufactured from the same alloy heat and billet stock. Their grain sizes, hardness values and  $\gamma''$  precipitate sizes and distributions are very similar. In spite of these similarities in their chemical compositions and microstructures their FCGR's differ markedly at 650°C in laboratory air, Fig. 11. It is therefore evident that the observed differences in their FCGR's arise primarily from the differences in their dislocation substructures. Higher FCGR's in the high TSN disc can be attributed to the presence of planar dislocation arrays because these planar arrays provide a favourable path for the growth of fatigue cracks. Similar observations have been made by Kendall, Hicks and King (15) in prestrained (5-7%) Incoloy 901. In contrast, cellular dislocation arrays in the medium TSN disc cause a reduction in the FCGR's relative to the high TSN disc. Hammond and Nutting (16) have suggested that pre-existing cellular dislocation arrays hinder the development of intense slip bands and thus reduce the amount of crack extension per fatigue cycle.

Dislocation substructures in turbine discs can be introduced either due to plastic deformation during forging or due to stress cycling during engine operation. Stress cycles associated with engine start-up, shut-down and major throttle excursions during service can lead to low cycle fatigue damage accumulation, i.e. plastic strain accumulation prior to crack initiation. The Alloy 718 discs examined in this study had been upset hammer forged at a starting forging temperature of 1050°C and the rim and the bore areas had been subjected to additional deformation at a starting forging temperature of 1000°C. The discs had then been partially solution treated well above the  $\gamma'$  solvus (871°C) or the  $\gamma''$  solvus (900°C) at 955°C for 1 hour. A partial solution treatment temperature of 955°C corresponds to 0.75 - 0.8  $T_m$  for the alloy. In the absence of intragranular  $\gamma'$  or  $\gamma''$  precipitates, the forging induced dislocation networks may either annihilate or rearrange to form a recrystallized grain structure because of the low stacking fault energy of Ni-base superalloys. Both discs revealed equiaxed recrystallized grain structures in the CT specimen locations, Fig. 13, indicating the absence of remnant forging

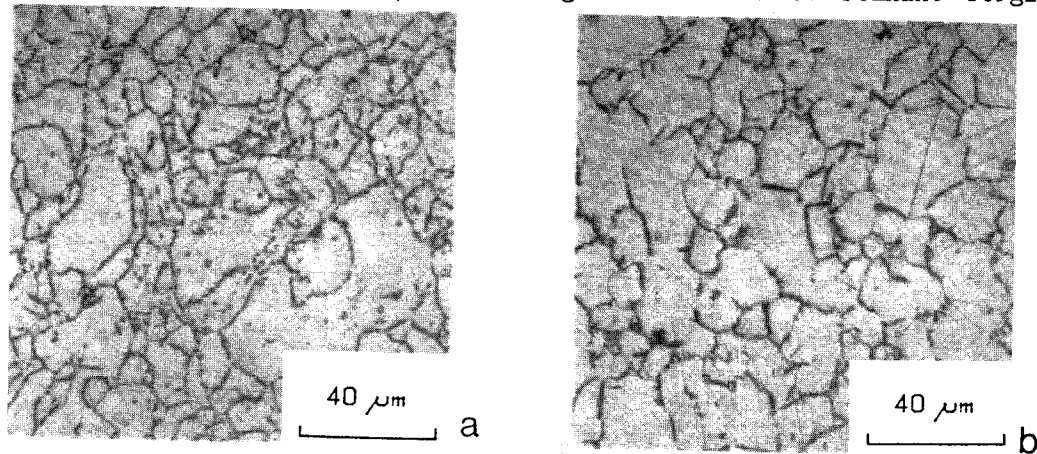


Fig. 13 Optical micrographs of Alloy 718 turbine discs in CT specimen locations. (a) High and (b) Medium TSN discs.

strains. Meetham (17), on the other hand, has shown that depending on the precise forging technique significantly different dislocation densities and distributions can be retained in Inconel 901. It is not clear from Meetham's paper whether these dislocation substructures were retained after the solution treatment of the alloy. Apparently, it is well recognized by the forging industry that dislocation substructures can significantly affect the service behaviour of highly stressed Ni-base superalloy turbine discs. Microstructures that are relatively dislocation free or contain homogeneous dislocation distributions behave satisfactorily whereas heterogeneous dislocation distributions in the form of high density planar arrays can result in premature component failure (17).

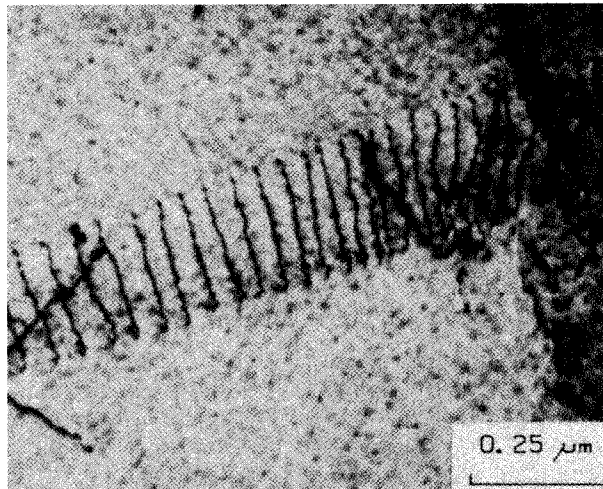


Fig. 14 Typical dislocation structures observed in virgin Alloy 718 forgings.

A number of conventionally heat treated Alloy 718 plates and bars from different material heats along with new disc forgings have previously been examined in the authors' laboratory (3,5,7). None of these materials have revealed the presence of planar dislocation arrays or subgrains of the type shown in Figs. 9a and 9b respectively. Instead, these materials always contained homogeneous dislocation distributions as shown in Fig. 14.

Electron microscopy of laboratory tested LCF specimens of typical turbine disc alloys such as Waspaloy and Alloy 718 has shown that microstructural features in the form of dense dislocation bands,  $\gamma'$  precipitate cutting, stacking faults associated with  $\gamma''$  precipitates, precipitation of additional phases and mechanical microtwins are generally present in the fatigued test coupons (18,19). Recent investigations by Rao et al (20) on LCF behaviour of Alloy 617 has however shown that microstructural damage can manifest itself in a variety of ways depending upon the strain rate and temperature conditions employed during strain controlled LCF testing. In low strain rate tests, Rao et al (20) observed subgrains formation similar to that shown in Fig. 9(b) in a majority of the grains in the LCF specimens. Antolovich and co-workers (21,22) have also observed subgrain formation in notched LCF specimens of Alloy 718 that were tested at very low strain ranges of the order of 0.05% at 427°C and the specimen lives were typically of the order of 40,000 cycles. It is therefore quite probable that the dislocation substructure observed in the service exposed discs were actually induced during service rather than being the result of the remnant forging strains.

It should be recognized that relative to the strain ranges operative in turbine discs during service, most laboratory investigations have been conducted at considerably higher strain ranges. Therefore, microdamage features observed in laboratory test coupons can be considerably different from those observed in actual components. Currently work is underway in the authors' laboratory to assess the evolution of LCF damage under realistic service strains in order to distinguish between the dislocation substructures produced by cyclic loading and remnant forging strains. It is quite conceivable that planar dislocation arrays and subgrains in the high TSN disc formed at a low strain amplitude, whereas the cellular dislocation structures formed at very low strain ranges. These details must be resolved prior to applying damage tolerance based life prediction concepts to turbine discs (9,23).

### Conclusions

1. A serrated grain boundary morphology improves the fatigue crack growth resistance of Alloy 718 at 650°C. Grain boundary serrations improve grain boundary strength and relieve boundary stress concentrations by suppressing grain boundary sliding. Serrated grain boundaries also provide a tortuous path for a growing crack under intergranular cracking conditions which in turn retards the crack growth rate.
2. Matrix dislocation substructures in service exposed Alloy 718 turbine discs substantially impact upon their FCGR resistance at 650°C. High dislocation densities in the form of planar dislocation arrays provide a favourable path for the growth of fatigue cracks. Relative to a cellular dislocation structure, the planar dislocation arrays increase the FCGR's by a factor of 2 to 5 over a  $\Delta K$  range of 30 to 55 MPa $\sqrt{m}$ .
3. Dislocation substructures in Alloy 718 turbine discs can form either due to remnant forging strains or due to stress cycling associated with engine start-up, shut-down and major throttle excursions. It is suggested that service induced LCF damage can produce a wide variety of substructures in this alloy and that their influence of FCGR's should be elucidated if damage tolerance concepts are used for the life cycle management of turbine discs.

### Acknowledgements

The authors would like to thank Dr. R. Thamburaj, Mr. M.R. Pishva and Mr. N.C. Bellinger of Hawker Siddeley Canada Inc. (previously with Carleton University) for their experimental contributions to this work. Useful discussions with Dr. S.D. Antolovich of Georgia Institute of Technology, Atlanta and Mr. J.M. Hyzak of Wyman-Gordon Company, MA are also greatly appreciated.

This work was conducted under NAE project 07D-subproject 07317: Aerospace Metallic Materials. The financial assistance for this work was provided by the Chief of Research and Development, Department of National Defence, Canada.

## References

1. K. Sadananda and P. Shahinian, 'Effect of Microstructure on Creep-Fatigue Crack Growth in Alloy 718', Res Mechanica, 1 (1980) 109 -128.
2. J.P. Pedron and A. Pineau, 'The Effect of Microstructure and Environment on The Crack Growth Behaviour of Inconel 718 Alloy at 650°C Under Fatigue, Creep and Combined Loading', Mat. Sci. and Eng. J., 56 (1982) 143 - 156.
3. R. Thamburaj, A.K. Koul, W. Wallace, T. Terada and M.C. deMalherbe, 'The Influence of Microstructure Upon the Creep and Fatigue Crack Growth Behaviour in Inconel 718', Proc. Conf. "Time-Dependent Fracture", 11th Canadian Fracture Conference, Ottawa, Canada, June 1984, Ed. A.S. Krausz, Martinus Nijhoff Publishers, pp 245 - 260.
4. W.J. Mills and L.A. James, 'Effect of Heat-Treatment Upon the Fatigue-Crack Growth Behaviour of Alloy 718 Weldments - Part II', J. of Eng. Mat. and Tech., 107 (1985) 41 - 47.
5. R. Thamburaj, T. Terada, A.K. Koul, W. Wallace and M.C. deMalherbe, 'The Influence of Microstructure and Environment Upon Elevated Temperature Crack Growth Rates in Inconel 718', Proc. Int. Conf. on Creep, Tokyo, Japan, April 1986, Eds. D. Woodford et al. ASME/JSME, pp 275 - 282.
6. D.D. Krueger, S.D. Antolovich and R.H. Van Stone, 'Effects of Grain Size and Precipitate Size on the Fatigue Crack Growth Behaviour of Alloy 718 at 427°C', Metall. Trans., 18A (1987) 1431 - 1449.
7. A.K. Koul, P. Au, N. Bellinger, R. Thamburaj, W. Wallace and J.-P. Immarigeon, 'Development of a Damage Tolerant Microstructure for Inconel 718 Turbine Disc Material', Proc. 6th Int. Symp. on Superalloys, Seven Springs, PA, Sept. 1988, 'Superalloy 88 Book', Eds. D.N. Duhl et al, pp 3 - 12.
8. H.F. Merrick, 'Effect of Heat Treatment on the Structure and Properties of Extruded P/M Alloy 718', Metall. Trans., 7A (1976) 505 - 514.
9. M.R. Pishva, A.K. Koul, N.C. Bellinger and T. Terada, 'Service Induced Damage in Turbine Discs and Its Influence on Damage Tolerance Based Life Predictions', Canadian Aeronautics and Space Journal, 35 (1989).
10. ASTM Standard Method E-647-83, 1985, 'Tentative Test Method for Constant Load Amplitude Fatigue Crack Growth Rates Above 10E-8m/Cycle', vol. 03.01, Philadelphia, U.S.A.
11. M.R. Pishva, N.C. Bellinger, T. Terada and A.K. Koul, 'DC-PD Technique for Crack Length Measurements at Elevated Temperatures', National Research Council of Canada Report, NRC-NAE LTR-ST-1635, October 1987.
12. R. Thamburaj, A.K. Koul, W. Wallace and M.C. deMalherbe, 'Effect of Microstructure and Environment on Creep and Fatigue Crack Growth Rates in Inconel 718', National Research Council of Canada Report, NRC-NAE LTR-ST-1586, May 1986.

13. D.A. Woodford, 'Environmental Damage of a Cast Ni-Base Superalloy', Metall. Trans., 12A (1981) 299 - 308.
14. M. Tanaka, H. Iizuka and F. Ashihara, 'Effects of Serrated Grain Boundaries on the Crack Growth in Austenitic Heat-Resistant Steels During HT Creep', J. of Mat. Sci., 23 (1988) 3827 - 3832.
15. J.M. Kendall, M.A. Hicks and J.E. King, 'The Effect of Prestraining on Fatigue Crack Growth Rates in Ni-Base Alloys', Fatigue 87, 1987.
16. C. Hammond and J. Nutting, 'The Physical Metallurgy of Superalloys and Titanium Alloys', in 'Forging and Properties of Aerospace Materials', The Metals Society, London, 1978, pp 75 - 102.
17. G.W. Meetham, 'Superalloy Processing and its Contribution to the Development of the Gas Turbine Engine', Proc. In Conf. 'High Temperature Alloys for Gas Turbines', Liege, Belgium, Sept. 1978, Eds. D. Coutouradis et al, Applied Science Publishers, London, pp 837 - 859.
18. M. Clavel and A. Pineau, 'Fatigue Behaviour of Two Ni-Base Alloys', Mat. Sci. and Eng. J., 55 (1982) 157 - 171.
19. B.A. Lerch, N. Jayaraman and S.D. Antolovich, 'A Study of Fatigue Damage Mechanisms in Waspaloy from 25 to 800°C', Mat. Sci. and Eng. J., 66 (1984) 151 - 166.
20. K.B.S. Rao, H. Schiffers, H. Schuster and H. Nickel, 'Influence of Time and Temperature Dependent Processes on Strain Controlled LCF Behaviour of Alloy 617', Metall. Trans., 19A (1988) 359 - 371.
21. S.D. Antolovich, 'Effect of Structural Instabilities on Mechanical Properties of Alloy 718', Present Conference Proceedings, 1989.
22. J. Theskin, 'The Effects of The Microstructure on The Notched LCF Response of Alloy 718 at 800°F', M.S. Thesis, University of Cincinnati, U.S.A., 1984.
23. A.K. Koul, R. Thamburaj, W. Wallace and M.C. deMalherbe, 'Practical Experience with Damage Tolerance Based Life Extension of Turbine Engine Components', Proc. AGARD-SMP Conf. on 'Damage Tolerance Concepts for Critical Engine Components', San Antonio, Texas, 1985, AGARD-CP-393, pp 23 - 1 to 23 - 22.